Miniaturization of Patch Antennas Using a Metamaterial-Inspired Technique

Raoul O. Ouedraogo, *Member, IEEE*, Edward J. Rothwell, *Fellow, IEEE*, Alejandro R. Diaz, Kazuko Fuchi, and Andrew Temme, *Student Member, IEEE*

***Abstract*—A new design methodology for producing highly miniaturized patch antennas is introduced. The methodology uses complementary split-ring resonators placed horizontally between the patch and the ground plane. By optimizing the geometry of the split rings, sub-wavelength resonance of the patch antenna can be achieved with a good impedance match and radiation characteristics comparable to those of a traditional patch antenna on a finite ground plane. Construction of the optimized antenna is straightforward, requiring only the sandwiching of two etched circuit boards. High levels of miniaturization are demonstrated through simulations and experiments, with reductions of a factor of more than four in transverse dimension achieved for a circular patch resonant at 2.45 GHz. Although miniaturization is accompanied by a decrease in antenna radiation efficiency and a loss of fractional bandwidth, antenna performance remains acceptable even for a 1/16 reduction in patch area.**

***Index Terms*—Antenna measurements, genetic algorithms, metamaterials, optimization, patch antenna.**

I. Introduction

THE demand for small, compact, low cost antennas has increased tremendously over the past years, due to the need for reduced antenna size in both military and commercial spheres. Microstrip patch antennas, though popular for these applications, are difficult to miniaturize since their resonant frequency is determined by the dominant mode of the patch cavity. Nevertheless, much work has been done to find ways to miniaturize patch antennas. One of the most common techniques is to use shorting plates [1] or shorting pins [2] to shift the voltage null away from the center of the patch. The level of miniaturization achieved with this technique depends on the placement position of the shorting element relative to the voltage null of the unloaded patch. By placing the shorting element at the edge of the patch, a maximum shift of the voltage null can be achieved and the transverse dimension of the antenna can be reduced by 60%.

Other well known miniaturization techniques involve placing slots on the radiating patch [3], [4] or fractalizing the radiating edge [5], thereby increasing the length of the current path and consequently reducing the resonant frequency of the antenna. The achievable level of miniaturization depends on the length of the extended current path, with a typical size reduction of about 38%. Folding the patch into a multi layered structure can be used to reduce the transverse dimension of the patch by 50% [6], but at the cost of increased thickness, such that the overall volume of the antenna is unchanged. Each of these methods is limited in the amount of miniaturization that may be achieved, and each is associated with a dramatic drop in radiation efficiency and a degradation of the radiation pattern in both the E and H planes.

Patch antennas can also be miniaturized by using a high permittivity or artificial dielectric substrate. Loading an empty patch cavity with a dielectric of relative permittivity ϵ_r produces a reduction in the resonant frequency proportional to $\sqrt{\epsilon_r}$. Readily available high permittivity dielectrics such as aluminum oxide $(\mathrm{Al_2O_3})$ provide a dielectric constant in the range $\epsilon_r \approx 10$ and thus may be used to produce size reductions of about 30–50% compared to conventional circuit board materials such as RT/duroid. Though dielectrics with much higher dielectric constants exist, their increased cost makes them unsuitable for low-cost consumer applications.

The emergence of new artificial materials such as high impedance surfaces (HIS), reactive impedance surfaces (RIS), magneto-dielectrics, and metamaterials provide new ways to achieve higher levels of miniaturization than more conventional techniques [7]–[20]. For instance, it is reported in [10] that an RIS can be used to both miniaturize (down to a size of $\lambda_0/10$) and increase the bandwidth of a patch antenna. However, the implementation of the RIS requires the use of high permittivity dielectrics ($\epsilon_r = 25$) and thick substrates (6 mm) to achieve the desired level of miniaturization and bandwidth. Unfortunately, the exorbitant cost of high permittivity dielectrics as well as the use of thick substrates render the RIS approach unsuitable for low-cost or low-profile applications. In [15], it is reported that sub-wavelength resonance of a patch antenna can be achieved by partially loading the patch cavity with a properly designed homogeneous, isotropic, negative permeability metamaterial. A practical implementation of this idea was later proposed in [16] and [17], where inclusions consisting of arrays of resonant structures such as split-ring resonators (SRRs) were used to create the required μ-negative medium. However, this implementation is problematic since several arrays of planar resonant structures must be oriented vertically within the patch cavity in order to be effectively excited by the horizontal dominant-mode magnetic field. Since the level of miniaturization achievable depends on the size and the number of inclusions (with larger inclusions producing lower resonant frequencies), very thick substrates are required to produce a meaningful reduction in

Manuscript received November 06, 2010; manuscript revised June 03, 2011; accepted November 23, 2011. Date of publication March 01, 2012; date of current version May 01, 2012. This work was supported by the National Science Foundation under Grant 0800388.

R. O. Ouedraogo, E. J. Rothwell, and A. Temme are with the Department of Electrical and Computer Engineering, Michigan State University, East Lansing, MI 48824 USA (e-mail: ouedraog@msu.edu; rothwell@egr.msu.edu).

A. R. Diaz and K. Fuchi are with the Department of Mechanical Engineering, Michigan State University, East Lansing, MI 48824 USA (e-mail: diaz@egr.msu.edu; fuchikaz@msu.edu; temmeand@msu.edu).

Digital Object Identifier 10.1109/TAP.2012.2189699

size. Additionally, the fabrication process of such structures results in high cost and complexity.

In [18]–[20] it is reported that by etching arrays of SRRs into the ground plane (creating complementary SRRs or CSRRs) it is possible to lower the resonant frequency of the patch to that of the CSRRs. However, this approach only provides modest size reductions (about 32% reported in [18]). Additionally, the presence of the array of large slots on the ground plane significantly reduces the front-to-back ratio (to almost 0 dB) while increasing the cross-polarization to the same level as the co-polarization in both E- and H-planes.

In this paper, a new design methodology is introduced to produce highly miniaturized patch antennas that are thin, low cost, and easy to fabricate. Importantly, miniaturization is accompanied by a very good impedance match, with a return loss of more than 20 dB in all cases, and without significantly compromising the radiation pattern. At least a 4.5 dB front-to-back ratio is maintained for a 75% size reduction, with excellent isolation between the co- and cross-polarized fields in both the E- and H-planes. There is a tradeoff, however, since increased levels of miniaturization result in a reduction of the bandwidth and radiation efficiency of the antenna. But even with a miniaturization to 1/16 the area of a traditional patch, the reductions in bandwidth and radiation efficiency remain acceptable.

Miniaturization is achieved by loading the patch cavity using complementary SRRs (CSRR). By duality with SRRs, these are excited by the vertical electric field of the patch cavity mode, and thus may be oriented horizontally between the patch and the ground plane. The geometry of the CSRR is optimized in place to produce appropriate antenna characteristics at frequencies much lower than the resonant frequency of the unloaded patch cavity. Since the size of the horizontal CSRR may be much larger than those used in [18]–[20], as well as the vertical inclusions used in [16] and [17] (up to the size of the ground plane), higher levels of miniaturization are possible. Moreover, the simple construction of the antenna and the use of low permittivity dielectric can lead to lower production cost compared to designs based on high permittivity dielectrics and other complex approaches using a HIS, RIS or magneto-dielectrics.

Preliminary simulations were used in [21] to explore the underlying principle of the patch miniaturization technique. The effectiveness of the proposed technique is demonstrated here with detailed discussions of the design, optimization procedure and the impact of the technique on the bandwidth, radiation efficiency, front-to-back ratio, and cross polarization of the antenna. Miniaturized antennas with a surface area reduction of more than a factor of 16 are achieved in simulations without serious degradation of impedance or pattern, and measurements of the performance of several prototypes are used to validate the results obtained from the simulations. Details of the design and the optimization procedure are provided next.

II. Basic Concept

Synthesis of μ-negative media was first demonstrated by Pendry *et al.* [22] using resonant structures such as SRRs. In [22] it is shown that by placing an array of properly designed SRRs in an environment where the magnetic field is polarized along the axis of the rings, the effective permeability of the resulting composite medium may be made to resonate at a frequency determined by the capacitance and inductance of the ring structure. The SRR can be made resonant at a much lower frequency by increasing its effective capacitance and inductance through the use of multiple concentric split rings as presented in [23]. In an alternative approach Falcone *et al.* [24] showed using the concepts of duality and complementarity, that the effective permittivity of a medium composed of CSRRs—annular slots cut into a conducting screen—can be tailored to desirable values if the medium is excited with an electric field polarized along the axes of the CSRRs. Given that the electric field of the dominant mode within a patch cavity is polarized normal to the ground plane, it is possible to excite properly designed CSRRs placed horizontally between the ground plane and radiating patch and thus lower the resonant frequency of the patch to that of the CSRRs. In a dual to the multiple concentric SRR approach of [23], the resonant frequency of a complimentary structure can be lowered by using multiple slots. Similarly, it is possible to maintain the resonant frequency of a complimentary structure while the dimensions of the screen are reduced by placing multiple concentric slots on the screen. This approach allows high levels of miniaturization of the CSRR with the highest level of miniaturization determined by the total number of slots that can be placed on the screen. By using an *in situ* optimization technique [25], the geometry of the CSRR within the patch cavity can be optimized by varying the number of slots and the dimensions of each slot to produce an antenna resonance at a frequency well below that of the unloaded antenna. Equivalently, the frequency of resonance can be kept fixed and the size of the loaded antenna can be reduced to desired levels of miniaturization. The use of the optimizer is crucial for finding CSRR geometries that couple well with the antenna to produce the desired output parameters. As is shown in the results section, several CSRR geometries can lead to the same frequency of resonance but produce different antenna reflection coefficients and efficiencies, many combinations of which are unacceptable.

III. Antenna Design

Fig. 1 illustrates the proposed geometry of a miniaturized circular patch antenna. A radiating circular patch is placed above a circular dielectric substrate backed by a circular ground plane of the same diameter as the substrate. A microstrip feed line is used to excite the patch. A conducting disk is placed horizontally between the patch and ground plane and complementary split-rings of various radii are created by removing metal from the disk. The geometry of the disk, shown in Fig. 2, is optimized by varying the number of complementary split rings, the radius of the largest ring, R_2, the slot width, W, the metallization width, S, and the gap width, G. To reduce optimization costs, the values of W, G, and S are chosen to be the same for all of the complementary split rings, and the radius of the disk, R_1, is set prior to optimization.

A. Proof of Concept Design

Consider a traditional patch antenna consisting of a circular copper patch of radius 23.1 mm etched on top of a circular

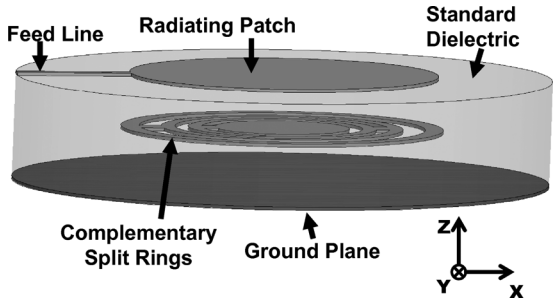

Fig. 1. Geometry of the miniaturized patch antenna.

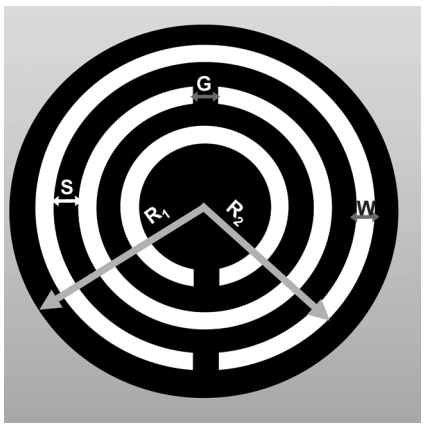

Fig. 2. Geometry of the disk containing the CSRR.

Rogers RT/duroid 5870 substrate of thickness 2.34 mm and radius 46.2 mm, backed by a copper ground plane also of radius 46.2 mm. The dielectric constant of the substrate is $\epsilon_r = 2.33$ and the dielectric loss tangent is $\delta = 0.0012$. Both dielectric and copper losses are included in the analysis of the performance of the antenna, and form the basis for determining the antenna radiation efficiency. A 50 Ω copper microstrip line of width 1.5 mm is used to feed the patch, with an SMA connector placed at the edge of the substrate. The radius of the patch is chosen such that the antenna resonates at 2.45 GHz. The goal of this design is to produce miniature versions of the antenna that achieve performance similar to the traditional patch at the 2.45 GHz operational frequency.

Three miniaturized patch antennas were designed. The radii of the patches were chosen to be 12 mm, 8 mm and 6 mm, which represent reductions in patch area to 1/4, 1/9, and 1/16, respectively, of the traditional patch (i.e., radius reduction of 1/2, 1/3, and 1/4). In each case, the ratio of patch radius to ground plane radius was held at 1:2, the substrate thickness was fixed at 2.34 mm, and the width of the microstrip line was kept at 1.5 mm to achieve a 50 Ω characteristic impedance; these are all identical to the corresponding properties of the traditional patch. Miniaturization was achieved by placing a copper disk containing a CSRR 0.78 mm below the radiating patch. The radius, R_1, of this disk in each case was chosen to be slightly smaller than the ground plane to avoid contact with the SMA connector. The values of R_1 used in each case are provided in Table I. Finally, the geometry of the CSRR was optimized in simulations using an in-house genetic algorithm (GA), as described next.

TABLE I
PARAMETER VALUES OF THE CSRR FOR EACH LEVEL OF MINIATURIZATION (DIMENSIONS IN mm)

Patch Radius	N	R_1	R_2	W	G	S
12	1	23	7.1	1.5	1.15	–
8	1	15	6.2	1.6	1.75	–
6	3	11.5	9.9	1.65	1.9	1.05

TABLE II
PARAMETER VALUES USED TO OPTIMIZE THE CSRR TO MINIATURIZE THE PATCH ANTENNA TO 1/4 AND 1/9 THE AREA OF THE TRADITIONAL PATCH (DIMENSIONS IN mm)

Parameter	Start	Step	End
R_2	5	0.15	14.45
G	0.1	0.075	2.425
S	0.3	0.1	3.4
W	0.3	0.1	3.4

TABLE III
PARAMETER VALUES USED TO OPTIMIZE THE CSRR TO MINIATURIZE THE PATCH ANTENNA TO 1/16 THE AREA OF THE TRADITIONAL PATCH (DIMENSIONS IN mm)

Parameter	Start	Step	End
R_2	5	0.1	11.3
G	0.1	0.075	2.425
S	0.3	0.075	2.65
W	0.3	0.075	2.65

B. Optimization Method and Analysis

The geometry of the CSRR appropriate for a desired level of miniaturization was determined in simulations by integrating the full wave solver HFSS with an in-house GA written in Matlab. The dimensional parameters R_2, W, S and G are encoded into a 21-bit binary string ρ, and the number of rings is determined by

$$N = \left\lfloor \frac{R_2}{S+W} \right\rfloor \tag{1}$$

where the floor operator $\lfloor x \rfloor$ rounds the positive number x to the largest integer less than x. For a given 21-bit binary string, the value of R_2 is determined by performing a binary to decimal conversion of the first six bits of the string. The values of W, S and G are determined by performing a similar conversion of the remaining 15 bits with 5 bits used for each parameter. The ranges of values allowed for each of the four parameters are shown in Tables II and III for each desired level of miniaturization.

The goal of the optimization is to produce a good impedance match without seriously compromising the radiation efficiency of the antenna. This is done by seeking low values of the cost function

$$F(\rho) = \eta_{\text{rad}} \times [20 \log_{10}(|S_{11}|)] \tag{2}$$

where $|S_{11}|$ is the magnitude of the reflection coefficient referenced to 50 Ω and η_{rad} represents the radiation efficiency of the antenna. The GA is configured for a 2-point crossover with an evolving single bit mutation. An initial population of 500 different binary strings is selected randomly and the corresponding antenna geometries are created in Matlab and exported to HFSS

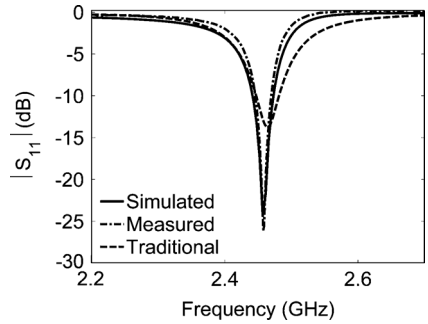

Fig. 3. Reflection coefficient of the patch antenna miniaturized to 1/4 the area of the traditional patch (traditional patch reflection coefficient added for reference).

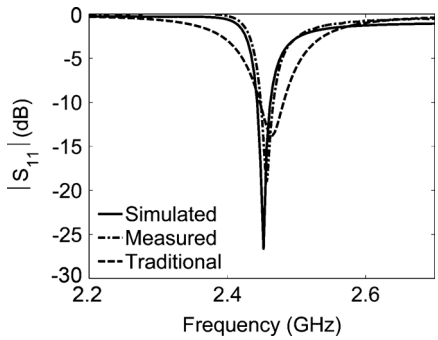

Fig. 4. Reflection coefficient of the patch antenna miniaturized to 1/9 the area of the traditional patch (traditional patch reflection coefficient added for reference).

for simulation. Note that only the geometry of the CSRR differs between simulation runs; the patch does not change. The cost of each binary string is then evaluated and ranked. The top 25% is selected for crossover and mutation until a new population of 100 binary strings (1/5 the starting population size) is generated. This process is repeated until the preset optimization goal of $20\log_{10}(|S_{11}|) < -10$ dB and $\eta_{\rm rad} > \gamma$ are reached. The value of γ is selected to be 1/2, 1/3 and 1/4 for the respective radii reductions to 1/2, 1/3 and 1/4. The time to complete a full-wave simulation for a given antenna geometry is approximately 150 seconds using an Intel Quad Core i7 computer.

IV. Results

For each desired level of miniaturization, the GA successfully found several sets of design parameters that produce a reflection coefficient lower than -10 dB. The parameters of the CSRR that produce the best identified cost values for each miniaturization level are provided in Table I, and frequency sweeps of the reflection coefficients for each optimized antenna are shown in Figs. 3–5 (a plot of the reflection coefficient of a traditional patch antenna designed on the same substrate is also shown in each figure for reference). It can be seen that a very good impedance match ($|S_{11}|$ less than -20 dB) is achieved for each desired level of miniaturization.

While it is to be expected that the bandwidth and the radiation efficiency of the miniaturized antennas will be reduced compared to the traditional patch antenna (due to the reduction in antenna volume), the properties of the three optimized antennas

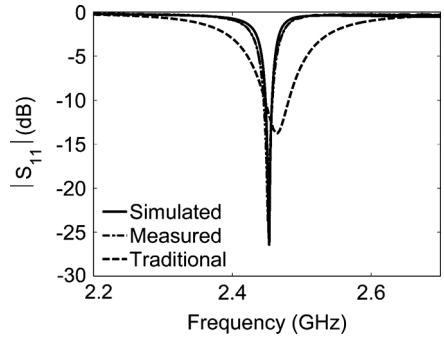

Fig. 5. Reflection coefficient of the patch antenna miniaturized to 1/16 the area of the traditional patch (traditional patch reflection coefficient added for reference).

remain quite good. From the simulations, the -10 dB bandwidths of the antennas with area reductions to 1/4, 1/9 and 1/16 of the traditional patch antenna are 1.2%, 0.81% and 0.4%, respectively, compared to 1.3% for the traditional patch antenna; the corresponding efficiencies are 84.7%, 49.8% and 28.1% respectively, compared to 94% for the traditional patch antenna.

A plot of reflection coefficient versus radiation efficiency obtained from the last generation of the GA used to miniaturize the patch area to 1/16 that of a traditional antenna is shown in Fig. 6. It can be seen that while several CSRR geometries produce patch antennas resonant at a given frequency, the performances of the antennas vary. The reflection coefficient ranges from below -25 dB to near 0 dB, while the radiation efficiency ranges from 10% to 80%. Note also that more than fifteen different CSRR geometries produce a reflection coefficient less than -10 dB, each with a different radiation efficiency. Some CSRR geometries produce reflection coefficients similar to those produced by the best structure found by the GA but with lower radiation efficiencies. This generally occurs with structures that have a larger number of slots than the best structure located by the GA. As an example, the parameters of a CSRR geometry for 1/16 area miniatiruization that produces a reflection coefficient of -23 dB and a radiation efficiency of 13.7%, compared to a reflection coefficient of -26 dB and a radiation efficiency of 28.1% for the best structure found, are shown in Table IV. It is seen that the best geometry loacted by the GA has three slots, while the geometry shown in Table IV has six slots. This suggests that using an overabundance of slots shifts the coupling of input power from the radiation mechanism to the loss mechanism, emphasizing the importance of using an optimizer to find the CSRR geometries that produce an acceptable combination of lower reflection coefficient and higher radiation efficiency.

The results shown in Fig. 6 are not exhaustive of all of the possible disk geometries, and thus the performance of the antennas presented here might not represent the best achievable using the proposed design methodology. Further GA optimizations involving the use of a different fitness function or different crossover and selection techniques may lead to better results. The use of a more sophisticated optimizer may also lead to better results.

When an SRR is placed in an environment with a time varying normal magnetic field, an electric current is induced

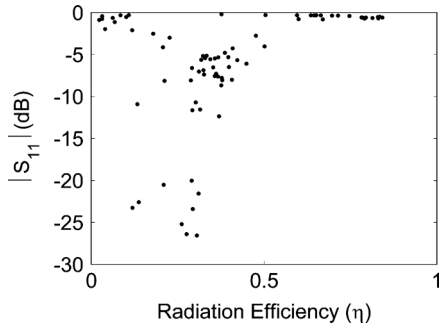

Fig. 6. Reflection coefficient vs. radiation efficiency of the last population for optimization of a patch antenna miniaturized to 1/16 the area of the traditional patch.

TABLE IV
PARAMETER VALUES OF A CSRR FOR 1/16 AREA MINIATURIZATION THAT PRODUCES A REFLECTION COEFFICIENT OF -23 dB AND A RADIATION EFFICIENCY OF 13.7% (DIMENSIONS IN mm)

Patch Radius	N	R_1	R_2	W	G	S
6	6	11.5	7.2	0.6	1.3	0.525

on the metal, reaching its peak at the frequency of resonance of the SRR. By duality, one would expect that a magnetic current is induced in the slots of a CSRR when the CSRR is placed in an environment with a time varying normal electric field. The magnetic current should reach its peak at the frequency of resonance of the CSRR. This effect is clearly seen in Fig. 7, which shows a plot of the intensity of the electric field on the surface of the CSRR disk for a resonant patch antenna miniaturized to 1/16 of the area of a traditional antenna. It can be seen that at resonance the electric field in the slots is very strong, with the intensity of the field greatest at the edges of the slots. This behavior is the expected edge singularity of the slot magnetic current. The intensity of the field is strongest in the middle slot, which has a diameter of $\lambda_0/9.6$. This diameter is comparable to those of the single slots found by the optimizer for patch areas of 1/4 and 1/9 of the traditional antenna (shown in Fig. 10). As the size of the conducting disk is reduced, more concentric slots must be created in order to maintain the same frequency of resonance and a good impedance match. Further optimizations to miniaturize the patch area to 1/64 that of a traditional antenna (resulting in a patch radius of 3 mm) produce a CSRR with five concentric slots and a reflection coefficient of -14 dB. Unfortunately, the radiation efficiency drops to only 5% and given that the ground plane is significantly reduced (to less than $\lambda_0/10$), the front-to-back ratio decreases to almost 0 dB.

The simulated E-plane and H-plane realized gain patterns of the various miniaturized patch antennas are shown in Figs. 8 and 9, respectively. The radiation patterns of the traditional patch antenna are also shown in these figures for comparison. Note from the two figures that the broadside nature of the radiation pattern is maintained in both planes, but the realized gain is reduced as the antenna is made smaller, primarily due to the decrease in radiation efficiency. Note also that the size of the backlobe increases as the antenna size is reduced, because the ground plane size is reduced in tandem with the patch. The smallest

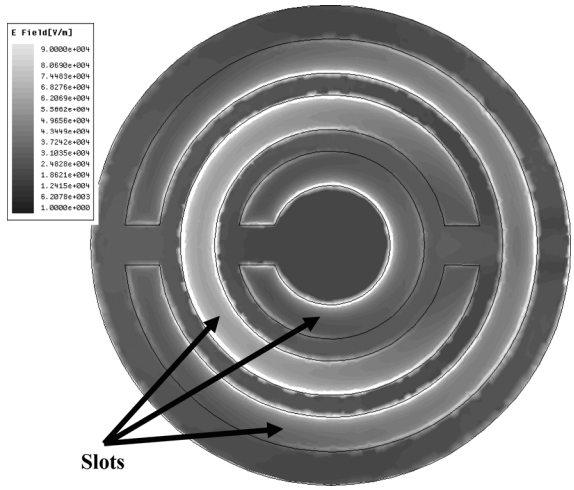

Fig. 7. Intensity of the electric field on the CSRR structure of the patch antenna miniaturized to 1/16 the area of the traditional patch.

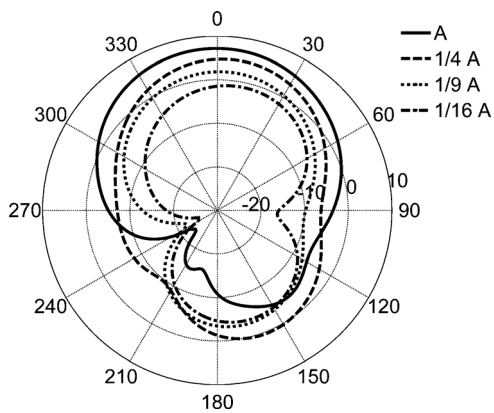

Fig. 8. Simulated E-plane realized gain patterns of the traditional and miniaturized patch antennas (10 dB/div). Size reduction is relative to the area of a traditional patch, A.

FBR is 4.5 dB and corresponds to the FBR of the antenna miniaturized to 1/16 the area of the traditional patch. This FBR is higher than the one reported in [16] (3 dB for an area reduction to 1/16) and [2] (2 dB for an area reduction to 1/9). The directivity of the miniaturized antennas remains very good as well despite the large reduction in antenna area. For instance, the directivity of the simulated antennas with area reductions to 1/4, 1/9 and 1/16 of the traditional patch antenna are 5.96 dB, 4.86 dB and 4.23 dB, respectively, compared to 7.34 dB for the traditional patch antenna. The isolation between the co-polarization minimum and cross-polarization maximum remains excellent (over 35 dB in the E-plane and 20 dB in the H-plane). The lack of symmetry of the E-plane (Fig. 8) is due to the presence of the microstrip feed and the CSRR gaps, which are aligned along the x axis as shown in Fig. 1. If desired, the asymmetry can be reduced somewhat by rotating the CSRR by 90 degrees.

The CSRR layer position is determined by available board thicknesses. The value of 0.78 mm used here is a standard substrate thickness manufactured by Rogers Corp. Additional optimizations with the CSRR placed 1.56 mm from the radiating patch produced results similar to those obtained for a distance of 0.78 mm. Note however that moving an optimized CSRR from

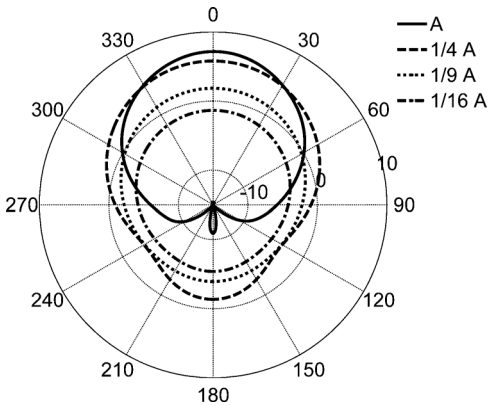

Fig. 9. Simulated H-plane realized gain patterns of the traditional and miniaturized patch antennas (10 dB/div). Size reduction is relative to the area of a traditional patch, A.

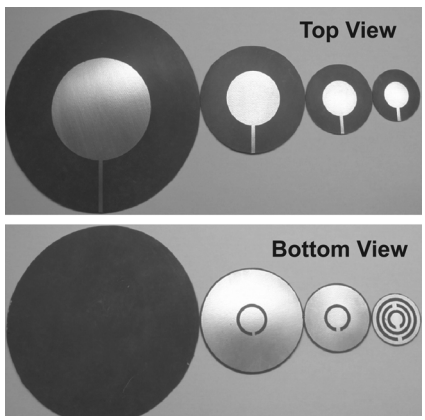

Fig. 10. First layer of the fabricated traditional circular patch antenna and miniaturized prototypes showing reductions to 1/4, 1/9, and 1/16 of the traditional patch area. The second layer, which includes the ground plane, is not shown.

the position where it was optimized alters the performance of the antenna, due to the change in coupling between the CSRR structure and its surroundings, and additional optimization would be needed to return the performance of the altered antenna to an acceptable level. It is also expected that antenna performance depends on the distance between the CSRR and the ground plane. This emphasizes the need for an optimizer to find appropriate CSRR structures for a given geometry.

Prototypes of the traditional and miniaturized antennas were fabricated through a photo etching process using a 0.78 mm thick double-sided Rogers 5870 duroid substrate and a 1.56 mm single-sided Rogers 5870 duroid substrate. The properties of the substrates are the same as those used in the simulations. The radiating patch was etched on one side of the 0.78 mm thick substrate and the CSRR was etched on the other side. The ground plane was provided using the single-sided 1.56 mm substrate. The final prototypes were produced by gluing the two substrates such that the CSRR is between the patch and the ground plane. The traditional patch was constructed the same way, except without the CSRR structures. Fig. 10 shows the top and bottom views of the etched 0.78 mm substrate.

The measured reflection coefficients of the miniaturized antennas are shown in Figs. 3–5, where they are compared to the

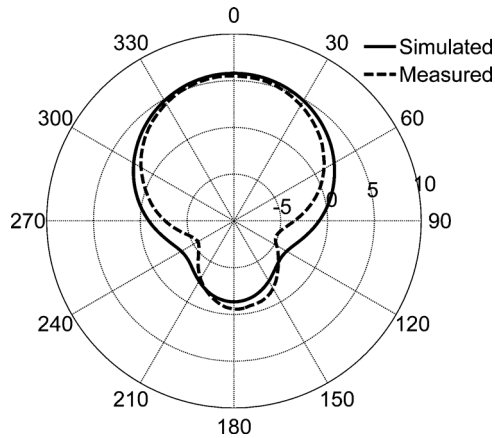

Fig. 11. Simulated and measured H-plane gain patterns of the patch antenna miniaturized to 1/4 the area of the traditional patch (5 dB/div).

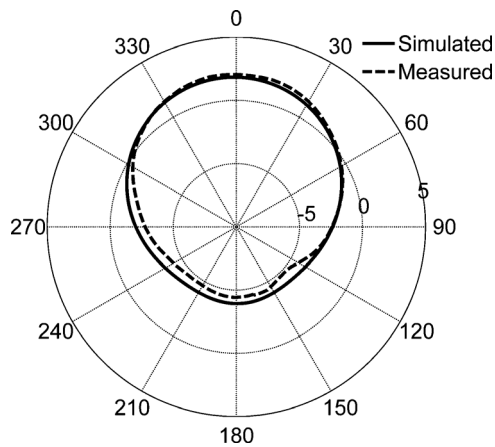

Fig. 12. Simulated and measured H-plane gain patterns of the patch antenna miniaturized to 1/9 the area of the traditional patch (5 dB/div).

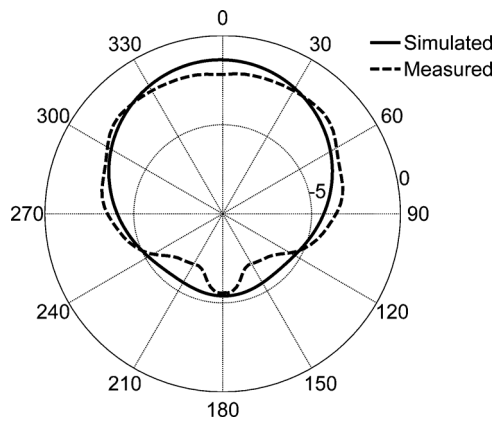

Fig. 13. Simulated and measured H-plane gain patterns of the patch antenna miniaturized to 1/16 the area of the traditional patch (5 dB/div).

results from simulations. In each case excellent agreement is seen between measurement and simulation. Figs. 11–13 compare the simulated and measured H-plane realized gain patterns of the miniaturized patch antennas. Good agreement is again observed between simulations and measurements, thus attesting to the feasibility of the proposed miniaturization technique.

V. Conclusion

A new design methodology for producing highly miniaturized patch antennas is introduced. By adding a single layer containing complementary split-ring resonators to a traditional patch structure, the size of the antenna can be reduced significantly while maintaining the impedance match and the structure of the field pattern. Because the construction is simple, the miniaturized antennas can be produced with little effort at low cost. Feasibility of the proposed technique has been validated by fabricating several miniaturized patch antennas with surface areas as small as one sixteenth that of a traditional patch antenna. Measurements of reflection coefficient and antenna pattern agree well with simulations. Even smaller antennas are possible, but with further size reduction comes a reduction in radiation efficiency and fractional bandwidth that may prove undesirable.

Note that although the work presented in this paper focuses on miniaturization of a circular patch antenna, the proposed design technique can also be applied to other patch geometries. Initial investigations performed using miniaturized rectangular patch antennas reveal performances similar to those found with circular patches. Also, preliminary results reveal that the proposed optimization technique may prove useful for producing patch antennas with multiband performance. This is currently being investigated in depth.

References

[1] K. L. Wong, *Compact and Broadband Microstrip Antennas*. Hoboken, NJ: Wiley, 2002.

[2] R. Waterhouse, "Small microstrip patch antenna," *Electron. Lett.*, vol. 31, no. 8, pp. 604–605, 1995.

[3] S. A. Bokhari, J. F. Zuercher, J. R. Mosig, and F. E. Gardiol, "A small microstrip patch antenna with a convenient tuning option," *IEEE Trans. Antennas Propag.*, vol. 44, no. 11, pp. 1521–1528, 1996.

[4] C. A. Balanis, *Modern Antenna Handbook*. Hoboken, NJ: Wiley, 2008.

[5] J. P. Gianvittorio and Y. Rahmat-Samii, "Fractal antennas: A novel antenna miniaturization technique, and applications," *IEEE Trans. Antennas Propag. Mag.*, vol. 44, no. 1, pp. 20–36, 2002.

[6] R. Chair, K. M. Luke, and K. F. Lee, "Miniature multi-layer shorted patch antenna," *Electron. Lett.*, vol. 36, no. 1, pp. 3–4, 2000.

[7] D. Sievenpiper, L. Zhang, R. F. J. Broas, N. G. Alexopoulos, and E. Yablonovitch, "High-impedance electromagnetic surfaces with a forbidden frequency band," *IEEE Trans. Microw. Theory Tech.*, vol. 47, pp. 2059–2074, 1999.

[8] D. Sievenpiper, H. P. Hsu, J. Schaffner, G. Tangonan, R. Garcia, and S. Ontiveros, "Low profile, four sector diversity antenna on high impedance ground plane," *Electron. Lett.*, vol. 36, pp. 1343–1345, 2000.

[9] K. Sarabandi, M. D. Casciato, and I. S. Koh, "Efficient calculation of the fields of a dipole radiating above an impedance surface," *IEEE Trans. Antennas Propag.*, vol. 50, pp. 1222–1235, 2002.

[10] H. Mosallaei and K. Sarabandi, "Antenna miniaturization and bandwidth enhancement using a reactive impedance substrate," *IEEE Trans. Antennas Propag.*, vol. 52, no. 9, pp. 2403–2414, 2007.

[11] P. M. T. Ikonen, K. N. Rozanov, A. V. Osipov, P. Alitalo, and S. A. Tretyakov, "Magneto-dielectric substrates in antenna miniaturization: Potential and limitations," *IEEE Trans. Antennas Propag.*, vol. 54, no. 11, pp. 3391–3399, 2006.

[12] K. Buell, H. Mosallaei, and K. Sarabandi, "A substrate for small patch antennas providing tunable miniaturization factors," *IEEE Trans. Microw. Theory Tech.*, vol. 54, no. 1, pp. 135–146, 2006.

[13] J. McVay, N. Engheta, and A. Hoorfar, "High-impedance metamaterial surfaces using Hilbert-curve inclusions," *IEEE Microw. Wireless Compon. Lett.*, vol. 14, no. 3, pp. 130–132, 2004.

[14] A. Erentok, P. Luljak, and R. W. Ziolkwoski, "Antenna performance near a volumetric metamaterial realization of an artificial magnetic conductor," *IEEE Trans. Antennas Propag.*, vol. 53, pp. 160–172, 2005.

[15] A. Alu, F. Bilotti, N. Engheta, and L. Vegni, "Sub-wavelength, compact, resonant patch antennas loaded with metamaterials," *IEEE Trans. Antennas Propag.*, vol. 55, no. 1, pp. 13–25, 2007.

[16] H. Mosallaei and K. Sarabandi, "Design and modeling of patch antenna printed on magneto-dielectric embedded-circuit metasubstrate," *IEEE Trans. Antennas Propag.*, vol. 55, no. 1, pp. 45–52, 2007.

[17] F. Bilotti, A. Alu, and L. Vegni, "Design of miniaturized metamaterial patch antennas with μ-negative loading," *IEEE Trans. Antennas Propag.*, vol. 56, no. 6, pp. 1640–1647, 2008.

[18] Y. Lee, S. Tse, Y. Hao, and C. G. Parini, "A compact microstrip antenna with improved bandwidth using complementary split-ring resonator (CSRR) loading," in *IEEE Int. Symp. Antennas and Propagation and URSI Radio Science Meeting Dig.*, 2007, pp. 5431–5434.

[19] A. U. Limaye and J. Venkataraman, "Size reduction in microstrip antennas using left-handed materials realized by complementary split-ring resonators in ground plane," in *IEEE Int. Symp. Antennas and Propagation and URSI Radio Science Meeting Dig.*, 2007, pp. 1869–1872.

[20] M. Li, M. Lu, and T. J. Cui, "Novel miniaturized dual band antenna design using complementary metamaterial," in *Metamaterials*, 2008, pp. 374–376.

[21] R. O. Ouedraogo and E. J. Rothwell, "Metamaterial-inspired patch antenna miniaturization technique," in *IEEE Int. Symp. Antennas and Propagation and URSI Radio Science Meeting Dig.*, 2010, pp. 1–4.

[22] J. B. Pendry, A. J. Holden, D. J. Robbins, and W. J. Stewart, "Magnetism from conductors and enhanced nonlinear phenomena," *IEEE Trans. Microw. Theory Tech.*, vol. 47, no. 11, pp. 2075–2084, 1999.

[23] F. Bilotti, A. Toscano, and L. Vegni, "Design of spiral and multiple split-ring resonators for the realization of miniaturized metamaterial samples," *IEEE Trans. Antennas Propag.*, vol. 55, no. 8, pp. 2258–2267, 2007.

[24] F. Falcone, T. Lopetegi, J. D. Baena, R. Marques, F. Martin, and M. Sorolla, "Effective negative-stop-band microstrip lines based on complementary split ring resonators," *IEEE Microw. Wireless Compon. Lett.*, vol. 14, no. 6, pp. 280–282, 2004.

[25] R. O. Ouedraogo, E. J. Rothwell, A. R. Diaz, S. Y. Chen, A. Temme, and K. Fuchi, "In situ optimization of metamaterial-inspired loop antennas," *IEEE Antennas Wireless Propag. Lett.*, vol. 9, pp. 75–78, 2010.

Raoul O. Ouedraogo (S'08–M'11) was born in Ouagadougou, Burkina Faso, in 1982. He received the B.Sc. degree from Southern Illinois University, Carbondale, IL, in 2006, the M.Sc. degree from Michigan State University, East Lansing, in 2008, and is currently working toward the Ph.D. degree at Michigan State University, all in electrical engineering.

His current research interests include metamaterials, small antennas, self-structuring devices, electromagnetic radiation, and scattering.

Edward J. Rothwell (F'05) was born in Grand Rapids, MI. He received the B.S. degree in electrical engineering from Michigan Technological University, Houghton, in 1979, the M.S. degree in electrical engineering and the degree of electrical engineer from Stanford University, Stanford, CA, in 1980 and 1982, and the Ph.D. degree in electrical engineering from Michigan State University, East Lansing, MI, in 1985, where he held the Dean's Distinguished Fellowship.

He worked for Raytheon Co., Microwave and Power Tube Division, Waltham, MA, from 1979 to 1982 on low power traveling wave tubes, and for MIT Lincoln Laboratory, Lexington, MA, in 1985. He has been at Michigan State University from 1985 to 1990 as an Assistant Professor of electrical engineering, from 1990 to 1998 as an Associate Professor, and from 1998 as Professor.

Dr. Rothwell received the John D. Withrow award for teaching excellence from the College of Engineering at Michigan State University in 1991, 1996 and 2006, the Withrow Distinguished Scholar Award in 2007, and the MSU Alumni Club of Mid Michigan Quality in Undergraduate Teaching Award in 2003. He was a joint recipient of the Best Technical Paper Award at the 2003 Antenna Measurement Techniques Association Symposium, and in 2005 he received the Southeast Michigan IEEE Section Award for Most Outstanding Professional. He is co-author of the book *Electromagnetics* (CRC Press, 2001). Dr. Rothwell is a Fellow of the IEEE, and a member of Phi Kappa Phi, Sigma Xi, and Commission B of URSI.

Alejandro R. Diaz received the Ph.D. degree in aerospace engineering in 1982 from the University of Michigan, after receiving B.S. and M.S. degrees also from the University of Michigan.

He is Professor and chair of the Department of Mechanical Engineering at Michigan State University (MSU). He joined the department in 1986 as assistant professor. Prior to coming to MSU, he was a research scientist at INTEVEP in Caracas, Venezuela. He was a visiting professor at the Technical University of Denmark in 1993.

Prof. Diaz is a Fellow of the American Society of Mechanical Engineers and Vice President of the International Society for Structural and Multidisciplinary Optimization.

Kazuko Fuchi was born in Kozakai, Japan, in 1984. She received the B.S. degree in physics from Michigan State University, East Lansing, MI, in 2008 and is currently working toward the Ph.D. degree at Michigan State University in mechanical engineering.

Her research interests include topology optimization of metamaterials and RF devices.

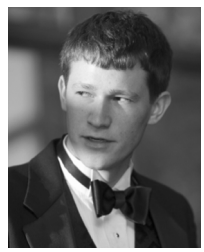

Andrew Temme (S'10) received the B.S. and M.S. degrees in electrical engineering from Michigan State University (MSU), East Lansing, MI, in May 2010 and December 2011, respectively. As an undergraduate, he worked in the Smart Microsystems Laboratory at MSU before joining the Electromagnetics Research Group in 2008 where he is currently.

His interests include through-wall radar, search and rescue, combustion, antenna design, and microwave measurement techniques.